UNIVERSITY OF
BATH

University of Bath

Hydrogen-Transfer Catalysis with Cp*Ir^{III} Complexes:

The Influence of the Ancillary Ligands

Ulrich Hintermair,†§* Jesús Campos,† Timothy P. Brewster,†# Lucas M. Pratt,† Nathan D. Schley,†‡ and

Robert H. Crabtree†*

† Department of Chemistry, Yale University, 225 Prospect Street, New Haven, Connecticut 06520, USA.

§ Centre for Sustainable Chemical Technologies, University of Bath, Claverton Down, Bath BA2 7AY,

UK.

Present address: Department of Chemistry, University of Washington, Seattle, Washington 98195,

USA.

‡ Present address: Division of Chemistry and Chemical Engineering, California Institute of Technology,

Pasadena, California 91125, USA.

§ u.hintermair@bath.ac.uk, †robert.crabtree@yale.edu

ABSTRACT

Fourteen Cp*Ir^{III} complexes bearing various combinations of N- and C- spectator ligands are assayed in hydrogen-transfer catalysis from *iso*-propanol to acetophenone under various conditions to investigate ligand effects in this widely used reaction. The new cationic complexes bearing monodentate pyridine and NHC ligands were characterized crystallographically and by VT-NMR. Control experiments and mercury poisoning tests showed that iridium(0) nanoparticles, although active in the reaction, are not responsible for the high activity observed for the most active precatalyst [Cp*Ir(IMe)$_2$Cl]BF$_4$ (**6**). Interestingly, for efficient catalysis it was found necessary to have both NHCs in monodentate form; tying them together in a bis-NHC chelate ligand gave greatly reduced activity. The kinetics of the base-assisted reaction showed induction periods as well as deactivation processes, and H/D scrambling experiments cast some doubt on the classical monohydride mechanism.

KEY WORDS

Transfer hydrogenation is a useful reduction protocol increasing in popularity, in part because these reactions can be run using a variety of liquid or solid hydrogen donors without the need for hydrogen gas.[1] Furthermore, the reversibility of the ionic H^+/H^- transfer[2] forms the basis for many useful C-C, C-O, and C-N bond forming reactions via 'borrowing-hydrogen' methodology.[3-6] The first catalytic systems mediating hydrogen transfer reported by Mitchell and Henbest[7-9] and Mestroni[10] were based on iridium compounds, and iridium catalysts are still amongst the most widely used today.[11] In the early 2000s, Ikariya and Noyori[12] and Fujita and Yamaguchi[13] introduced half-sandwich Cp*Ir complexes (including chiral versions[14-16]) as easily accessible and versatile precatalysts, which have quickly found wide use.[17] More recently, some Cp*Ir-NHC complexes (NHC = N-heterocyclic carbene) have been shown to be particularly effective.[18-20] Several Cp*Ir precatalysts are currently commercially available, and the first examples are moving towards industrial application.[21]

The commonly accepted mechanism of Cp*Ir-catalyzed hydrogen transfer follows the 'monohydride route' assuming full retention of all ancillary ligands.[22] Although this pathway represents a reasonable scenario in analogy with other transition-metal based catalysts it fails to fully account for the influence of ligand effects in the Cp*Ir precursors,[23] partly because the kinetics are still rather poorly understood. Here we present a systematic study of a small library of Cp*Ir complexes with non-functional[24] C- and N- donor spectator ligands in hydrogen-transfer catalysis to investigate ligand effects in this important transformation. In this paper, we focus on the effect of the ancillary ligands around the Cp*Ir fragment while in a future contribution we will look at the role of the Cp* ligand. A highlight of the present work is the development of a new, highly active Cp*Ir precatalyst that may follow a different mechanism from that commonly assumed for this type of precursor.

Complexes **1-14** (Figure 1) were designed as catalyst precursors to probe the influence of pyridines versus NHCs (**1** *vs.* **2** *vs.* **3**, **4** *vs.* **5** *vs.* **6**, **8** *vs.* **10** *vs.* **11**), chelating versus mono-dentate (**4** *vs.* **11**, **5** *vs.* **10**, **6** *vs.* **8**), LL-type versus LX-type (**10** *vs.* **13**, **11** *vs.* **14**), and remote pH-switchable ligands (**10** *vs.* **12**).
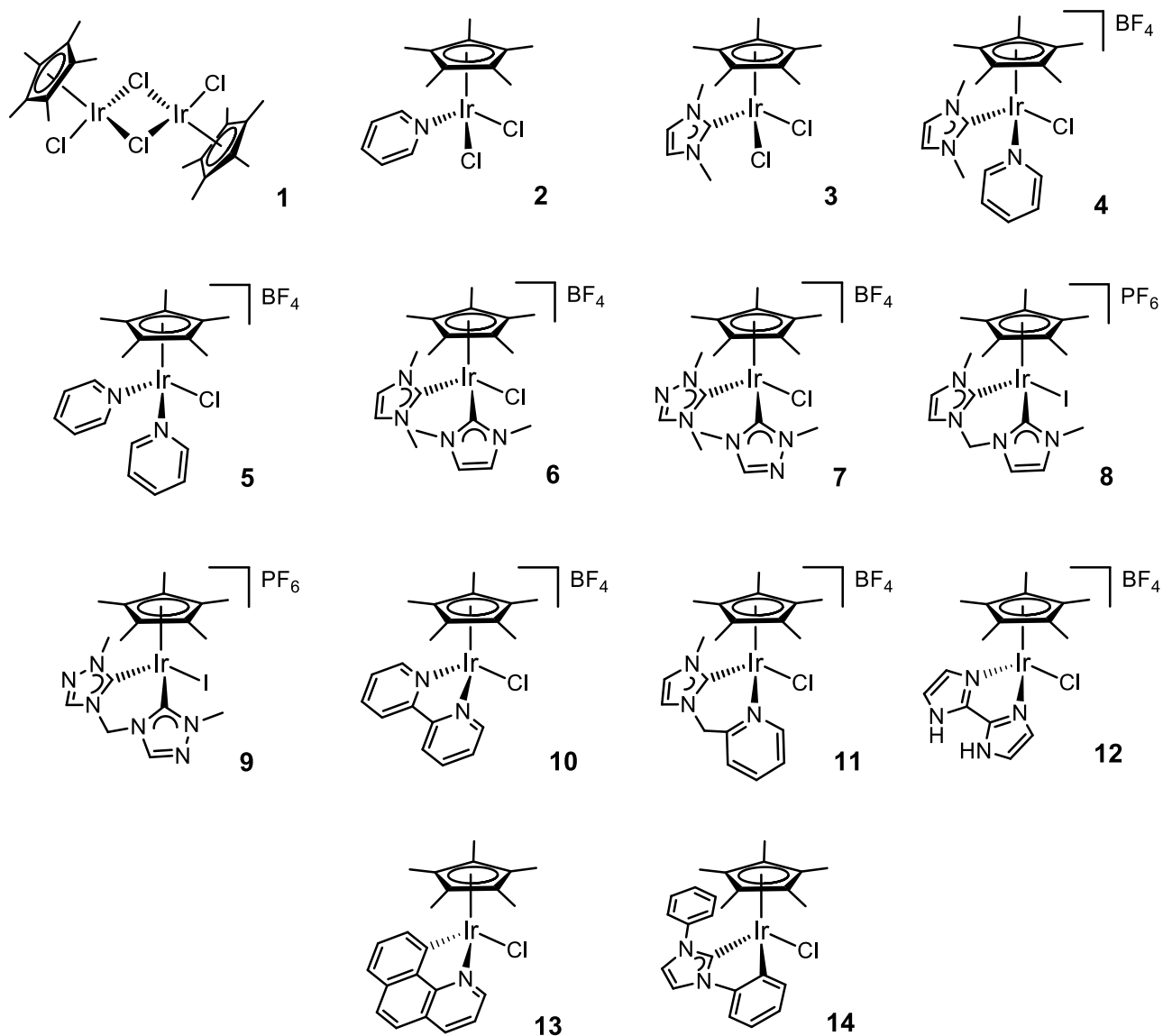

Figure 1. Cp*Ir^{III} complexes evaluated in transfer-hydrogenation catalysis.

The reactivity switch of Ag-NHC complexes from mono-NHC transfer to bis-NHC transfer as a function of the coordination ability of the anion described previously for transmetalation reactions with Rh[I] and Ir[I] complexes[25] was also found to apply to [Cp*IrCl$_2$]$_2$, and allowed convenient access to mono- and bis-NHC complexes **3, 6**, and **7**, respectively (Scheme 1 and Figure 2). All other compounds were obtained via slight modifications of known procedures and isolated in good to excellent yields as air- and moisture-stable, crystalline solids after purification (see Experimental Section).

Scheme 1. Single NHC transfer (left) versus double NHC transfer with anion metathesis (right) at [Cp*IrCl$_2$]$_2$ depending on the Ag-NHC complex used (Z = halide, X = weakly coordinating anion).

0.5 [Ag(NHC)Z]$_2$
−AgZ

3
96 % (known)

0.5

[Ag(NHC)$_2$]X
−AgCl

6
91 % (new)
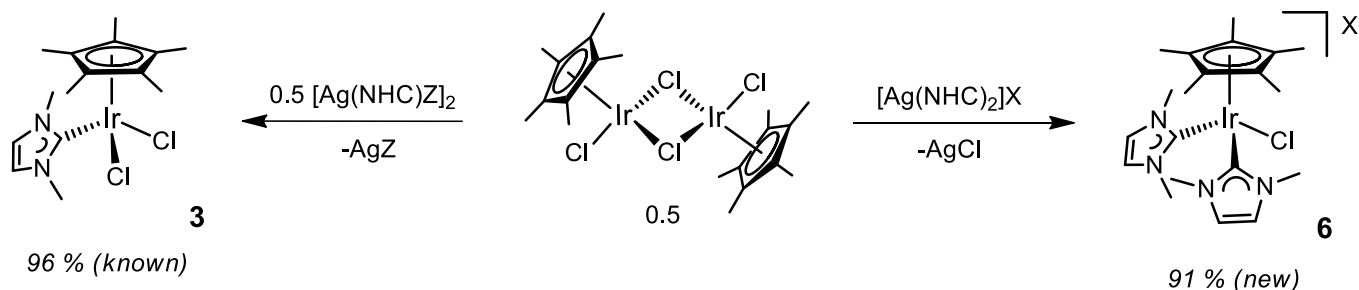
Compounds **4, 5, 6, 7, 9**, and **12** have been characterized by single-crystal X-ray diffraction (Figure 2) while crystal structures of **3**,[26] **8**,[27] **10**,[28] **11**,[26] **13**[29] and **14**[30] have been reported previously. In the solid state, all complexes have the expected piano-stool geometry without any unexpected features. As summarized in Table 1, ligand bite angles and bond lengths are very similar in the chelating and monodentate cationic complexes.
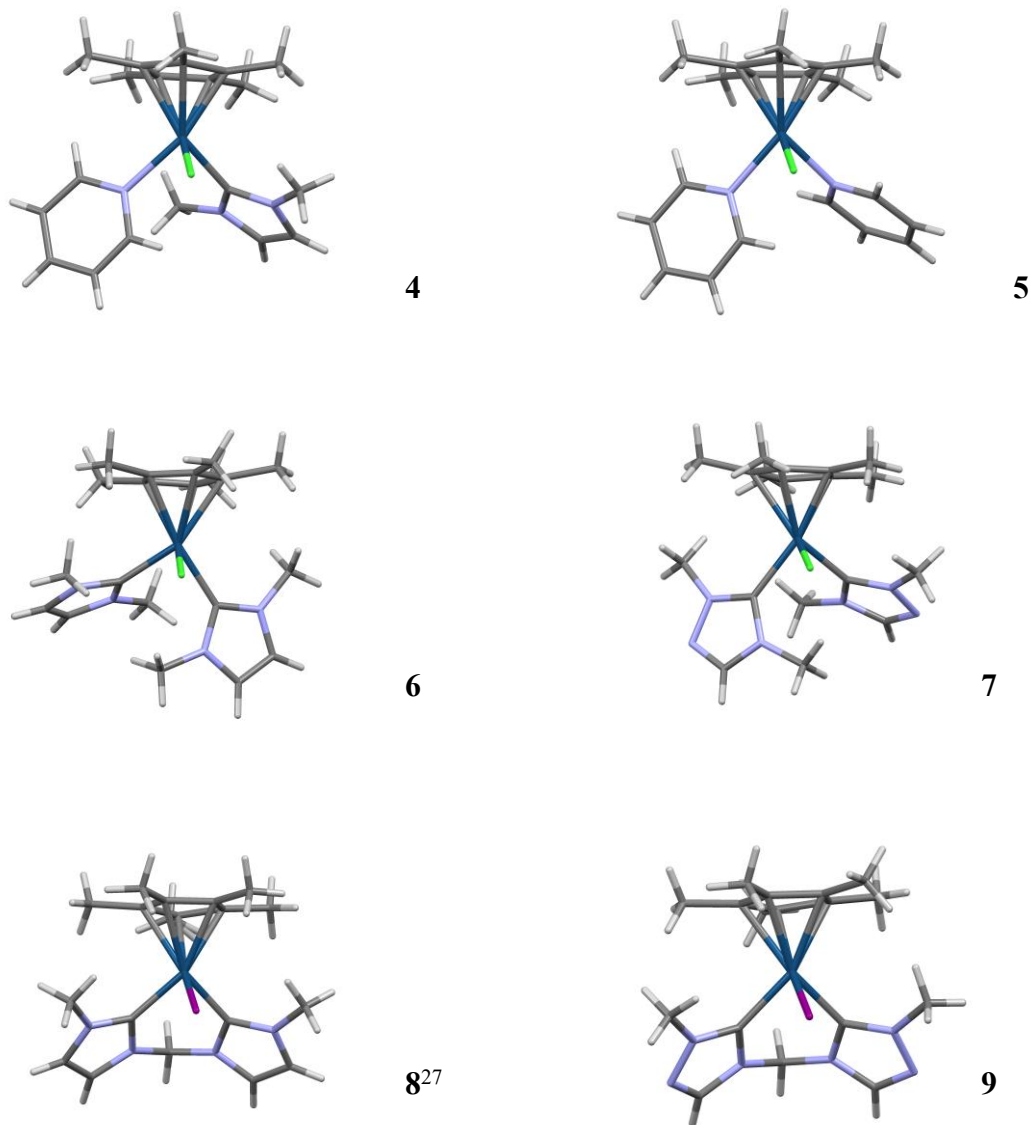
Figure 2. X-ray crystal structures of complexes **4**, **5**, **6**, **7**, **8**[27] and **9** (counterions and solvent molecules omitted for clarity)

**Table 1.** Comparison of selected structural data of Cp*Ir complexes in the solid state.

complex	Ir-L distances	L-Ir-L angles
4	2.08 Å (C), 2.16 Å (N)	87.3°

5	2.16 Å	83.9°
6	2.06 Å	86.1°
7	2.05 Å	85.0°
8[27]	2.02 Å	86.4°
9	2.04 Å	85.0°
10[28]	2.10 Å	76.1°
11[26]	2.02 Å (C), 2.10 Å (N)	85.4°
12[31]	2.11 Å	75.4°
13[29]	2.06 Å (C), 2.10 Å (N)	78.8°
14[30]	2.00 Å (NHC), 2.05 Å (aryl)	77.6°

In solution, both the pyridines and the minimally substituted IMe (1,3-dimethylimidazol-2-ylidene) and TMe (1,4-dimethyl-1,2,4-triazol-5-ylidene) ligands were found to rotate freely around the L-M axis on the NMR timescale at room temperature even in the bis-ligated complexes **4-7**, indicating little steric hindrance. Variable-temperature ^{1}H NMR at 500 MHz in CD_2Cl_2 showed decoalescence of the IMe signals in **6** below 223 K, and decoalescence of the TMe in **7** below 233 K (see Supporting Information). In the mixed py/IMe complex **4** the IMe ligand peaks split below 248 K, while the pyridine ligand gave one set of sharp peaks down to 193 K (see Supporting Information).

Freshly purified complexes **1-14** were evaluated for activity in the transfer-hydrogenation of acetophenone at 1 mol% [Ir] loading after 3 hours in refluxing ^{i}PrOH (~82 °C) under N_2 (Scheme 2). Reactions were run in the presence of 10 mol% KOH, 2 mol% $AgBF_4$, or without any additional promoter. Conversions were determined by ^{1}H-NMR spectroscopy using 1,3,5-trimethoxybenzene as internal standard.

Scheme 2. Transfer-hydrogenation of acetophenone to *rac*-1-phenylethanol from excess *iso*-propanol.
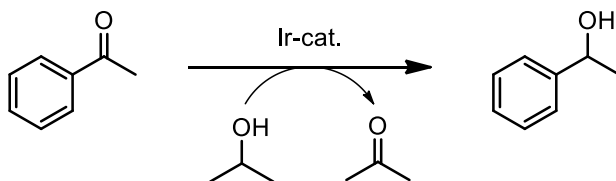
As can be seen from Figures 3-5, conversion to product varied widely depending on the conditions applied and precatalyst used. With the assistance of 10 mol% KOH, most precatalysts afforded significant conversion except complexes **8**, **9**, **12**, and **14**. Interestingly, the simple [Cp*IrCl$_2$]$_2$ precursor **1** outperformed many of the more sophisticated Cp*Ir complexes, although **6** and **10** were clearly the most effective precatalysts under these conditions. Using Ag$^+$ as activating agent instead of a base gave lower conversions and different trends in activity. Complexes **4** and **5**, bearing a labile pyridine base, gave the best results of ~70 % conversion under these conditions. Attempted double-activation with KOH and AgBF$_4$ gave virtually zero activity for all complexes (data not shown). A black precipitate formed in all of these reactions, suggesting *in-situ* formation of Ag$_2$O that effectively removes both Ag$^+$ and OH$^-$ from the solution. Without any additive, activities were very low (<5 %) for all precursors except **5** and **11** (~15% conversion), as expected for precursors with non-functional spectator ligands.

Figure 3. Activity of complexes **1-14** in the transfer-hydrogenation of acetophenone (Scheme 2). Reaction conditions: 2 mmol substrate, 1 mol% [Ir], 10 mol% KOH, 3 mL ^{i}PrOH, reflux, N_2, 3 hours (^{1}H NMR analysis with 1,3,5-trimethoxybenzene as internal standard, triplicates).

Figure 4. Activity of complexes **1-14** in the transfer-hydrogenation of acetophenone (Scheme 2). Reaction conditions: 2 mmol substrate, 1 mol% [Ir], 2 mol% AgBF$_4$, 3 mL ^{i}PrOH, reflux, N_2, 3 hours (^{1}H NMR analysis with 1,3,5-trimethoxybenzene as internal standard, duplicates).
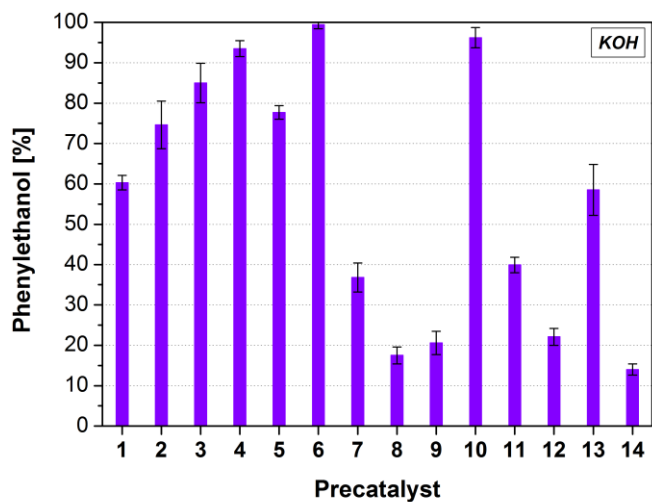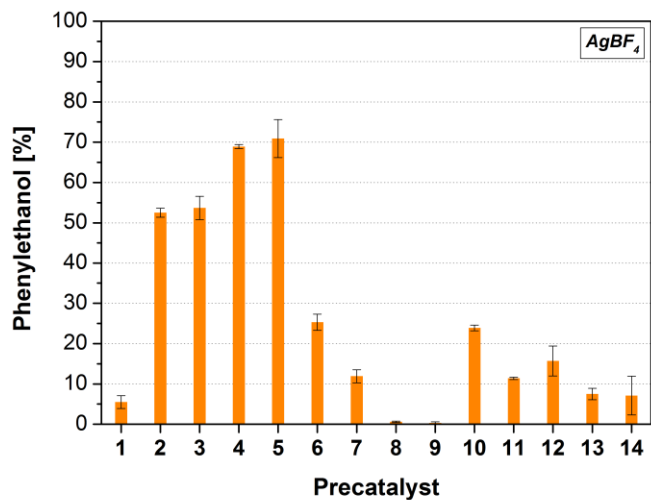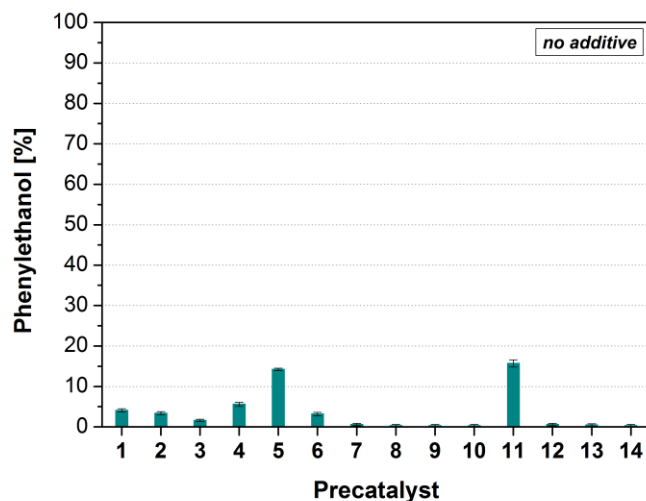
Figure 5. Activity of complexes **1-14** in the transfer-hydrogenation of acetophenone (Scheme 2). Reaction conditions: 2 mmol substrate, 1 mol% [Ir], 3 mL ^{i}PrOH, reflux, N_2, 3 hours (^{1}H NMR analysis with 1,3,5-trimethoxybenzene as internal standard, duplicates).

The base-assisted reactions were found to be sensitive to both oxygen and moisture. No conversion was observed when running the catalysis in air, and addition of 50 μL water (~140 eq. with respect to [Ir]) under N_2 equally shut down all activity. The addition of activated 3Å MS to the reaction did not improve performance either, however. In acidic aqueous media (10-100 eq. HOTf or HClO$_4$ in 1:1-10:1 iPrOH/H$_2$O) even the most active precursor **6** was completely inactivated, in contrast to aqueous hydrogen transfer reactions with Cp*Ir precatalysts using formate as the reductant, where optimum activity is typically observed in acidic media (pH~2 for NH$_4$COOH, pH~3 for NaCOOH).[32]

As the base-assisted reactions were the most efficient, we examined the background reactivity of KOH alone under our conditions. Transfer-hydrogenations of aldehydes and ketones are known to be slowly catalyzed by simple alkali metal bases,[33-35] and even alcohol alkylations can be achieved with base only.[36] Following activity over time showed that about 16 % phenylethanol was produced by 10 mol%

KOH after 3 hours at 80 ºC (Figure 6), indicating that complexes **8**, **9**, **12**, **14** had effectively afforded zero activity (Figure 3). Lowering the temperature to 60 ºC gave much lower base-catalyzed activity of only ~2 % after 4 hours, and at 40 ºC no product could be observed by ^{1}H NMR even after 12 hours.
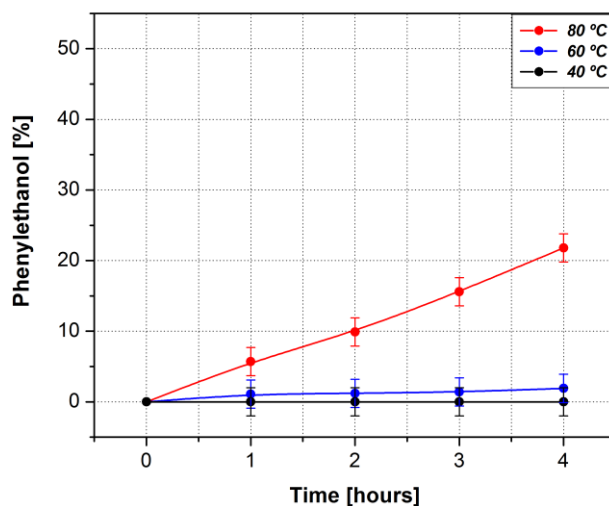

Figure 6. Background activity of KOH (10 mol%, semiconductor grade) in the transfer-hydrogenation of acetophenone at different temperatures (2 mmol substrate, 3 mL ^{i}PrOH, N$_2$; ^{1}H NMR analysis with 1,3,5-trimethoxybenzene as internal standard; lines drawn to guide the eye).

Next, some simple iridium compounds, including heterogeneous forms, were evaluated in the reaction to test for potential contributions from decomposition products of the Cp*Ir precursors (Table 2). Numerous heterogeneous catalysts,[37] including IrO$_2$,[38] and various metal nanoparticles (NPs) are known to catalyze transfer-hydrogenations quite efficiently,[39-44] and for some related iron and ruthenium complexes metallic NPs have recently been shown to contribute to catalytic activity.[45,46] *In-situ* de-ligation of molecular precursors to give heterogeneous material as the true active species is a persistent ambiguity in homogeneous catalysis often responsible for misleading ligand effects.[47]

Table 2. Activity of various iridium compounds in the transfer-hydrogenation of acetophenone (Scheme 2).[a]

precatalyst	with KOH	no additive
$IrCl_3 \times 3\ H_2O$	$81 \pm 2\ \%$	$7 \pm 1\ \%$
IrO_2 (powder)[b]	$21 \pm 3\ \%$	$0\ \%$
Ir/C (0.5 wt%)[b]	$29 \pm 11\ \%$	$0\ \%$
2-3 nm Ir^0 NPs[48]	$94 \pm 6\ \%$	$4 \pm 1\ \%$

[a] 2 mmol substrate, 1 mol% [Ir], 3 mL ^{i}PrOH, reflux, N_2, 3 hours (^{1}H NMR analysis with 1,3,5-trimethoxybenzene as internal standard, duplicates). [b] dried at 80 ˚C in vacuo for at least 3 hours prior to use.

As expected from the early work of Mitchell and Henbest,[9] $IrCl_3$ hydrate afforded good activity with >80 % conversion in 3 hours, surpassing many of the Cp*Ir precursors under identical conditions (cf. Figure 3). While IrO_2 and iridium on carbon barely added to the background activity of KOH, iridium(0) nanoparticles synthesized *in-situ*[48] prior to catalysis were highly active in the presence of base (Table 2). These findings might at first appear indicative of Ir NPs being the true catalyst in all cases, with the activity trends merely reflecting the ease of reductive *in-situ* decomposition. We therefore ran reactions with Ir NPs, $IrCl_3$, and **6** in the presence of excess Hg to selectively poison heterogeneous forms of metallic iridium[49] (Table 3). While the preformed NPs were effectively deactivated by Hg, both $IrCl_3$ and **6** displayed virtually unperturbed activity in its presence, strongly suggesting genuine solution-phase catalysis in case of the molecular precursors.[50]

Table 3. Mercury poisoning test of different iridium precatalysts in the transfer-hydrogenation of acetophenone (Scheme 2).[a]

precatalyst	no Hg	with Hg
6	99 ± 1 %	98 ± 1 %
$IrCl_3 \times 3\ H_2O$	39 ± 1 %	37 ± 1 %
2-3 nm Ir NPs[48]	64 ± 1 %	5 ± 1 %

[a] 2 mmol substrate, 1 mol% [Ir], 10 mol% KOH, 3 mL ^{i}PrOH, 60 ºC, N_2, 3 hours (^{1}H NMR analysis with 1,3,5-trimethoxybenzene as internal standard).

After having subtracted background reactivity of the base and provided evidence against *in-situ* decomposition into heterogeneous catalysts, we can discuss the activities of the most active precursors $IrCl_3$, **1 – 6**, and **10** in comparison with the less active ones. Clearly, both IMe and pyridine are good supporting ligands for Cp*Ir transfer-hydrogenation catalysts, but no obvious trends regarding ligand denticity, sterics, or electronics are apparent from this data set collected under strictly comparable conditions. For example, linking the two pyridines in **5** to give a bipy ligand in **10** slightly increases catalyst activity, whereas the same strategy has a much opposed effect in the case of two IMe in **6** versus **8** or one IMe and one pyridine as in **4** versus **11**. Also, going from IMe to TMe, a subtle change in electronics,[51] dramatically decreases catalyst activity in **7** as compared to **6**. Further decreasing the ligand donor power by moving to **5** and **10** gave intermediate activity. Only one discernible trend emerged: assuming **12** was deprotonated under reaction conditions, one could conclude that LX-type chelate ligands are inferior to LL-type combinations.

In view of the surprisingly high performance of the unlinked bis-NHC complex **6**, we monitored the reaction progress of $IrCl_3$, **1**, **3**, and **6** by *in-situ* ^{1}H NMR at lower temperature to compare the effects of

13

introduction of the Cp* and IMe ligands (Figure 7). At 60 ºC, IrCl₃ was barely active (20 % conversion after 3 hours), but introducing the Cp* ligand (**1**) caused a marked increase in activity (70 % conversion after 3 hours). Further introduction of one IMe ligand to the Cp*Ir fragment (**3**) decreased activity again, whereas introduction of the second IMe ligand (**6**) boosted catalyst activity to afford full conversion in less than 2 hours. This striking difference in performance of **3** and **6** demonstrates that both monodentate IMe ligands in **6** are needed for efficient transfer-hydrogenation catalysis and suggests their retention during turnover.
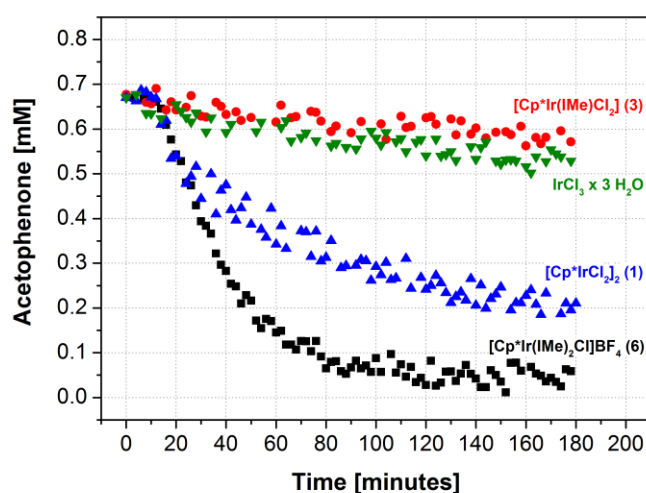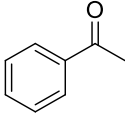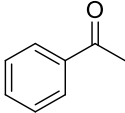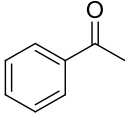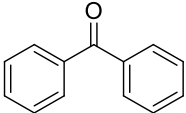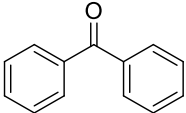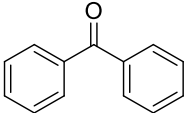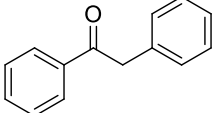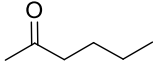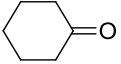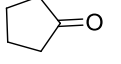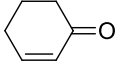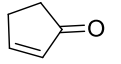

Figure 7. Activity of different iridium precatalysts in the transfer-hydrogenation of acetophenone (Scheme 2). Reaction conditions: 0.67 mmol substrate, 1 mol% [Ir], 10 mol% KOH, 1 mL ^{i}PrOH, 60 ºC, N₂ (*in-situ* ^{1}H NMR analysis with 1,3,5-trimethoxybenzene as internal standard).

We then further explored the transfer-hydrogenation scope of **6**. At 1 mol% loading, full conversion of various aromatic and aliphatic ketones was achieved within 3 hours at 60 ºC (Table 4). α,β-unsaturated ketones (entries 11 & 12) were found to be completely reduced to the saturated alcohols with >90 % conversion. In refluxing *iso*-propanol, **6** still afforded activity at 0.01 mol% loading to reach turnover numbers beyond 3000 after 6 hours (entries 3 & 6).

14

Table 4. Performance of precatalyst **6** at different loadings in the transfer-hydrogenation of various substrates from ^{i}PrOH.[a]

entry	mol% of **6**	substrate	conversion	TON
1 [b]	1.0		99 ± 1 %	99 ± 1
2	0.1		99 ± 1 %	990 ± 10
3 [c]	0.01		31 ± 1 %	3100 ± 100
4 [b]	1.0		99 ± 1 %	99 ± 1
5	0.1		99 ± 1 %	990 ± 10
6 [c]	0.01		23 ± 1 %	2300 ± 100
7 [b]	1.0		99 ± 1 %	99 ± 1
8 [b]	1.0		99 ± 1 %	99 ± 1
9 [b]	1.0		99 ± 1 %	99 ± 1
10 [b]	1.0		99 ± 1 %	99 ± 1
11 [b]	1.0		94 ± 1 % [d]	94 ± 1 (×2) [d]
12 [b]	1.0		95 ± 1 % [d]	95 ± 1 (×2) [d]

[a] 2 mmol substrate, 10 mol% KOH, 3 mL ^{i}PrOH, reflux, N$_2$, 3 hours (^{1}H NMR analysis with 1,3,5-trimethoxybenzene as internal standard). [b] at 60 ºC. [c] after 6 hours. [d] complete reduction to saturated alcohol.

In search of a rationale for the observed ligand effects, the kinetics of the acetophenone reduction with **6** were investigated. Variation of the KOH loading with 1 mol% [Ir] at 60 ºC showed that the rate was clearly base-dependent with slower turnover at lower base loading (Figure 8), but due to the sigmoidal shape of the reaction profile, kinetic analysis with respect to the order in base could not be performed. As before (Figure 7), a non-productive lag phase of several minutes was always observed which was virtually unaffected by the amount of KOH present. Nevertheless, high conversions were still reached after longer reaction times at lower base loading, which may be beneficial for the reduction of sensitive substrates where time is less important.
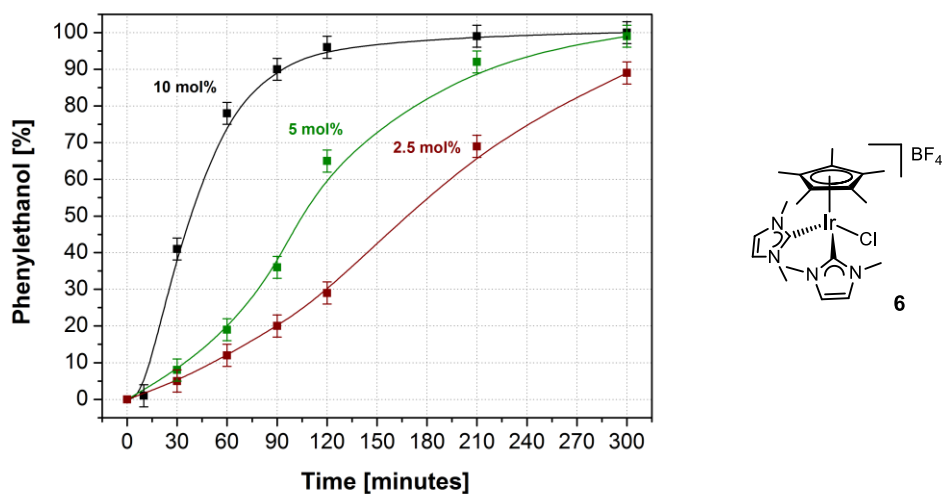
Figure 8. Activity of **6** in the transfer-hydrogenation of acetophenone (Scheme 2) at various loadings of KOH. Reaction conditions: 2 mmol substrate, 1 mol% [Ir], 3 mL ^{i}PrOH, 60 ºC, N_2 (^{1}H NMR analysis with 1,3,5-trimethoxybenzene as internal standard; lines drawn to guide the eye).

Varying the concentration of **6** at a fixed KOH loading of 10 mol% showed that both the length of the non-productive lag phase and the rate of acetophenone reduction were strongly dependent on the iridium concentration (Figure 9).
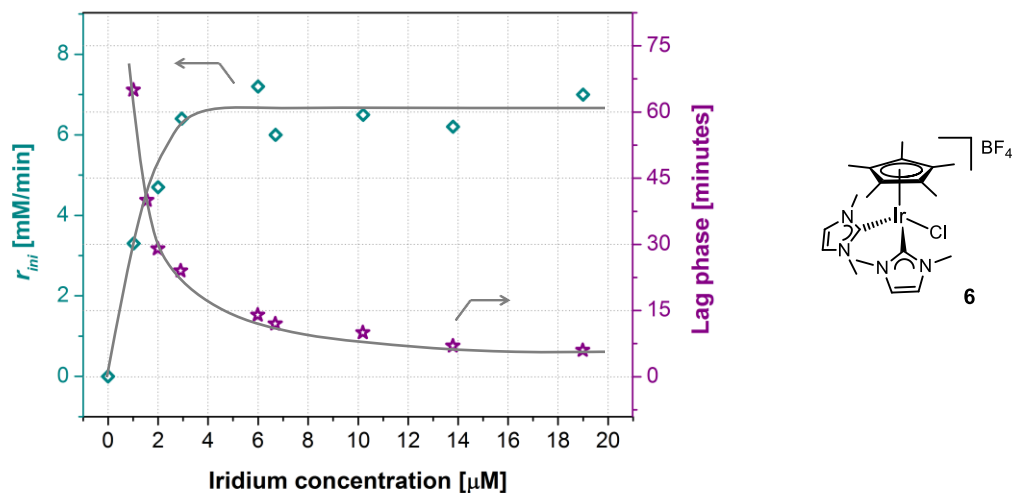
Figure 9. Lag phases (stars, right axis) and approximate initial rates (diamonds, left axis) of the transfer-hydrogenation of acetophenone (Scheme 2) by **6** at various catalyst loadings. Reaction conditions: 0.67 mmol substrate, 10 mol% KOH, 1 mL ^{i}PrOH, 60 °C, N$_2$ (*in-situ* ^{1}H NMR analysis with 1,3,5-trimethoxybenzene as internal standard; lines drawn to guide the eye).

The lag phase dependence on [Ir] cleanly followed second order kinetics with an apparent rate constant of k_{obs} = 61 µM^{-1}min^{-1}, suggesting a pre-catalytic activation step involving two iridium centers (Figure 10). The rates at the onset of catalysis, which could be estimated at 10 mol% base (cf. Figure 8), showed two distinct kinetic regimes. Below ~4 µM [Ir], the initial rate of acetophenone reduction after the lag phase was clearly dependent on [Ir], whereas at higher concentrations an apparent zero-order regime prevailed. Limiting base/Ir ratios were ruled out by testing catalysis at 6.7 µM **6** (= 1 mol%) with 25 mol% base instead of the usual 10 mol% (as in Figures 7 and 8), which gave no further increase in the rate of acetophenone reduction. Therefore, we suspect an [Ir]-dependent catalyst deactivation process after pre-activation to be responsible for the apparent rate saturation above ~4 µM [Ir].[52] With such complex kinetics it is not surprising that our understanding of ligand effects in Cp*Ir precatalysts for these transformations is still so limited despite their extensive use.
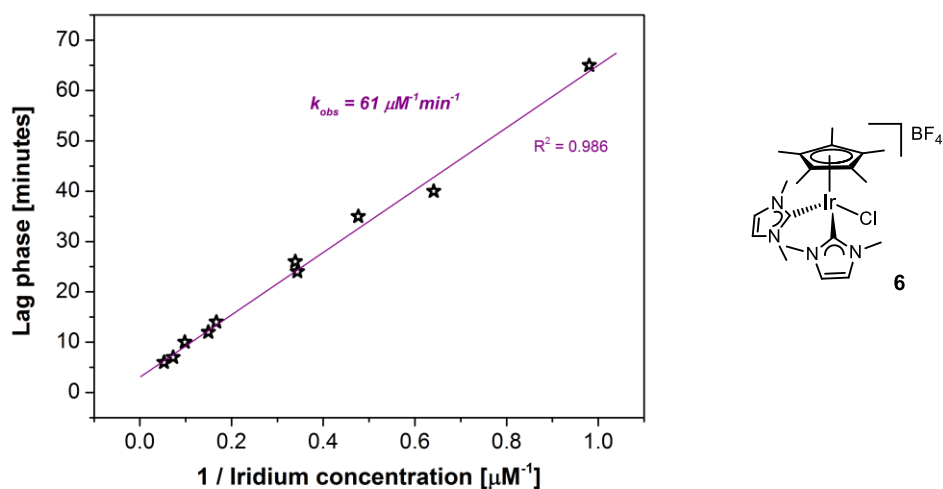
Figure 10. Second-order dependence of the duration of non-productive lag phases in the transfer-hydrogenation of acetophenone (Scheme 2) by **6** on iridium concentration. Reaction conditions: 0.67 mmol substrate, 10 mol% KOH, 1 mL ^{i}PrOH, 60 °C, N_2 (*in-situ* ^{1}H NMR analysis with 1,3,5-trimethoxybenzene as internal standard).

The commonly accepted mechanism of base-assisted transfer-hydrogenations from *iso*-propanol with Cp*Ir complexes follows the so-called 'monohydride' route, in which the base shuttles the protic hydrogens between the alkoxides and the iridium catalyst delivers the hydrides from the carbinol to the carbonyl carbons (Scheme 3).[23]

Scheme 3. Commonly accepted hydrogen delivery scheme in the monohydride mechanism of base-assisted transfer-hydrogenation catalysis.[23]
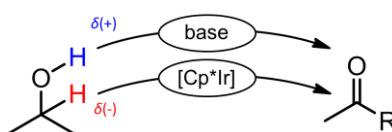
Accordingly, Cp*Ir-monohydride complexes are considered key intermediates in these reactions.[18,23] We thus synthesized the corresponding monohydride complex of **6** by reaction with sodium borohydride, which gave the desired compound **6-H** as colorless solid in high yield (Scheme 4). The complex was found to be air and moisture stable and inert towards reductive elimination of HIMe$^+$ or halide exchange with chlorinated solvents at ambient temperature.

Scheme 4. Synthesis of monohydride complex **6-H** (see Experimental Section for details).
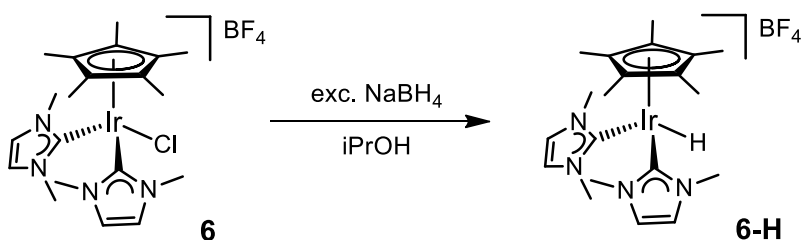
The ^{1}H NMR resonance of the terminal hydride in **6-H** at -16.24 ppm (in CD$_2$Cl$_2$) lies in the expected range by comparison with similar complexes reported previously.[53-56] Using the same reaction protocol with complex **7**, only traces of the putative hydride **7-H** could be detected by ^{1}H NMR at -15.74 ppm in the crude reaction mixture and no stable product could be isolated. Complex **8**, however, successfully yielded the stable monohydride derivative **8-H** (-15.98 ppm)[27] after silver-assisted iodide abstraction (see Experimental Section). Both **6-H** and **8-H** proved active in base-assisted transfer-hydrogenation of acetophenone (Table 5), in contrast to [Cp*Ir(NHC)(H)$_2$] (-16.9 ppm) and [Cp*Ir(NHC)(μ-H)]$_2^{++}$ (-17.4 ppm) complexes, which have been reported to be inactive and thus suspected relevant to catalyst deactivation pathways.[18] The inner-sphere chloride version **8**(Cl) of the iodide complex **8** was also prepared[27] for direct comparison with the chloride complex **6** and their corresponding hydrides. As can be seen from Table 5, the more strongly binding iodide had only a small inhibiting effect on activity in transfer hydrogenation catalysis.

Table 5. Comparison of halide and monohydride complexes in the transfer-hydrogenation of acetophenone (Scheme 2).[a]

precatalyst	conditions	conversion
6(Cl)	60 °C, 1 hour	78 ± 1 %
6-H		56 ± 1 %
8(I)	reflux, 3 hours	18 ± 2 %
8(Cl)		43 ± 1 %
8-H		73 ± 1 %

[a] 2 mmol substrate, 1 mol% [Ir], 10 mol% KOH, 3 mL ^{i}PrOH, N$_2$, (^{1}H NMR analysis with 1,3,5-trimethoxybenzene as internal standard).

Although this simple activity comparison of halide versus monohydride complexes in case of **6** and **8** did not allow to comment on their role in the catalytic cycle, it is worth mentioning that the monohydrides **10-H** (-11.80 ppm)[57] and **13-H** (-14.98 ppm)[58] are also known to be stable but only **10-H** has been reported to be active in transfer-hydrogenation catalysis.[57] Bäckvall's test for monohydride pathways was then applied by following acetophenone reduction from 99 % (CD$_3$)$_2$CD-OH by ^{1}H NMR using **6** and **6-H** to quantify the degree of H/D scrambling during hydrogen transfer (Scheme 5).[22]

Scheme 5. Bäckvall's H/D scrambling test to probe the number of hydrides in the active species of transfer-hydrogenation (cf. Scheme 3).[22] Note that kinetic isotope effects may lead to > 50 % D transfer to the carbinol in the polyhydride mechanism, but would not affect the selectivity of the monohydride mechanism.[59]

100 % D to carbinol
= selective transfer with retention of H⁺/D⁻ polarization
-> indicative of monohydride species

50 % and less D to carbinol
= unselective transfer with scrambling of H⁺/D⁻
-> indicative of polyhydride species
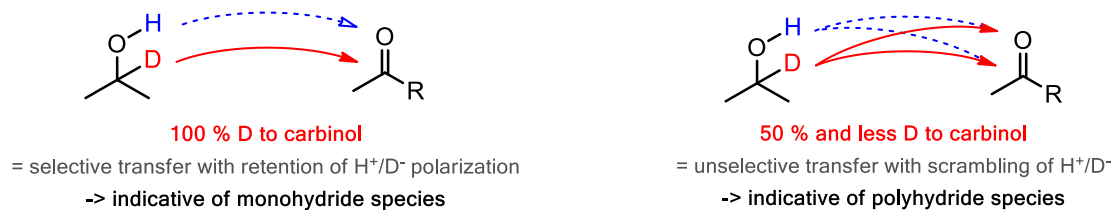
At 1 mol% [Ir] with 10 mol% KOH at 60 ºC, the chloride complex **6** incorporated 75 % D at the carbinol of phenylethanol, whereas for the hydride **6-H** 95 % D incorporation at the same position were seen by *in-situ* ^{1}H NMR. In both cases, the levels of product deuteration remained constant throughout the reaction up to 90 % conversion as quantified against 1,3,5-trimethoxybenzene as internal standard (see Experimental Section for details). Thus, while **6-H** gave products consistent with the classic monohydride route, **6** gave an inconclusive result as to the number of metal hydrides involved, suggesting that **6-H** may not be the only possible hydride intermediate in catalysis with **6**.

21

We have synthesized and characterized a number of new Cp*Ir complexes bearing combinations of pyridine and NHC ligands, and compared their activity in transfer–hydrogenation catalysis to structurally related literature compounds under various conditions. Contributions from the base and potential heterogeneous forms of iridium have been examined separately, and mercury poisoning experiments showed the Cp*Ir systems to be homogeneous. Complex **6** bearing two monodentate IMe ligands emerged as the most active precatalyst for the reduction of acetophenone from *iso*-propanol in the presence of KOH, surprisingly superior to its chelating bis-NHC congener. At lower temperatures of 60˚ C, **6** reduces a variety of ketone substrates with full conversion within two hours, reaching TONs >3000 at 0.01 mol% loading. Reaction progress monitoring in comparison with the mono-NHC complex **3** showed that both NHCs are needed for efficient catalysis. The kinetics of the catalysis with **6** were complex, showing a bimolecular activation period followed by base-dependent hydrogen-transfer catalysis with an apparent rate saturation at [Ir] concentrations >4 µM. A stable monohydride derivative of **6** has been synthesized which is active in the reaction, but H/D scrambling data suggest that it may not be the only intermediate in the catalytic cycle. Although the mechanistic reason for the superiority of **6** and the role of the monohydride in catalysis remain to be examined further in a following report, the present work provides important insight into this basic transformation and sheds some light on ligand effects in these widely used Cp*Ir precatalysts.

General. Organic solvents were purified by passing over activated alumina with dry N_2. All chemicals were purchased from major commercial suppliers and used as received. Syntheses were performed under an inert atmosphere of dry N_2 using standard Schlenk techniques. NMR spectra were recorded on either 400 MHz or 500 MHz Bruker Avance spectrometers and referenced to residual protio-solvent signals. The chemical shift δ is reported in units of parts per million (ppm). MS analyses were performed by the Mass Spectrometry and Proteomics Resource of the W.M. Keck Foundation Biotechnology Resource Laboratory at Yale University. [1,3-dimethylimidazolium]BF_4 and [1,4-dimethyl-1,2,4-triazolium]BF_4,[60] [Cp*IrCl$_2$]$_2$ (**1**),[61] [Cp*Ir(IMe)Cl$_2$] (**3**),[26] [Cp*Ir(bis-IMe)I]PF_6 (**8**),[27] [Cp*Ir(bis-TMe)I]PF_6 (**9**),[62] [Cp*Ir(bipy)Cl]BF_4 (**10**),[28] *rac*-[Cp*Ir(py-IMe)Cl]BF_4 (**11**),[26] [Cp*Ir(biim)Cl]BF_4 (**12**),[31] *rac*-[Cp*Ir(bequi)Cl] (**13**),[29] and *rac*-[Cp*Ir(phe-IPh)Cl] (**14**)[30] were synthesized via slightly modified literature procedures. Single crystals suitable for X-ray crystallography were obtained by diffusion of Et_2O into concentrated CH_2Cl_2 solutions at room temperature. Details of the X-ray diffraction experiments can be found in the Supporting Information.

[(η^5-pentamethylcyclopentadienyl)Ir^{III}(κN-pyridine)Cl$_2$] (2). [Cp*IrCl$_2$]$_2$ (120 mg, 0.15 mmol) was dissolved in CH_2Cl_2 (10 mL) and pyridine (24 mg, 0.3 mmol) added, causing an immediate color change from orange to yellow. After stirring at room temperature for 15 minutes the solvent was evaporated under reduced pressure, yielding a yellow-orange powder that did not change color upon drying *in vacuo*. Yield = 140 mg (98 %). ^{1}H-NMR (400 MHz, CD_2Cl_2): δ = 8.92 (dd, J = 6.5 Hz, J = 1.6 Hz, 2H, *o*-CH^{py}), 7.77 (tt, J = 7.7 Hz, J = 1.6 Hz, 1H, *p*-CH^{py}), 7.37 (ddd, J = 7.7 Hz, J = 6.5 Hz, J = 1.6 Hz, 2H, *m*-CH^{py}), 1.49 (s, 15H, C$_5$(CH_3)$_5$). ^{13}C{^{1}H}-NMR (100 MHz, CD_2Cl_2): δ = 153.7 (s, *o*-CH^{py}), 138.3 (s, *p*-CH^{py}), 125.9 (s, *m*-CH^{py}), 86.1 (s, C_5(CH$_3$)$_5$), 8.6 (s, C$_5$(CH$_3$)$_5$). ESI(+)MS calcd for $C_{15}H_{20}ClIrN^+$ (**2** - Cl): 440.089, 442.091. Found: m/z = 440.318, 442.313.

***rac*-[(η^5-pentamethylcyclopentadienyl)Ir^{III}(κC-1,3-dimethylimidazol-2-ylidene)(κN-pyridine)Cl]BF$_4$ (4).** [Cp*Ir(IMe)Cl$_2$] (**3**, 99 mg, 0.2 mmol) was dissolved in CH$_2$Cl$_2$ (10 mL) and pyridine (19 mg, 0.24 mmol) added. Upon addition of AgBF$_4$ (39 mg, 0.2 mmol) in MeOH (1 mL) the mixture turned bright yellow with immediate precipitation of a colorless solid. After stirring at room temperature for one hour the solid was filtered off, discarded, and the clear solution dried *in vacuo* to leave a yellow solid. Recrystallization from acetone/Et$_2$O gave yellow microcrystals. Yield = 106 mg (85 %). ^{1}H-NMR (400 MHz, CD$_2$Cl$_2$): δ = 8.46 (d, J = 5.3 Hz, 2H, *o*-CH^{py}), 7.93 (t, J = 7.4 Hz, 1H, *p*-CH^{py}), 7.40 (t, J = 6.7 Hz, 2H, *m*-CH^{py}), 7.13 (s, 2H, NCHCHN), 3.51 (bs, 6H, NCH_3), 1.66 (s, 15H, C$_5$(CH_3)$_5$). ^{13}C{^{1}H}-NMR (100 MHz, CD$_2$Cl$_2$): δ = 155.0 (s, *o*-CH^{py}), 154.4 (s, NCN), 139.2 (s, *p*-CH^{py}), 127.3 (s, *m*-CH^{py}), 125.0 (s, NCHCHN), 91.9 (s, *C$_5$*(CH$_3$)$_5$), 38.2 (s, NCH$_3$), 9.5 (s, C$_5$(*C*H$_3$)$_5$). ESI(+)MS calcd for C$_{15}$H$_{23}$ClIrN$_2^+$ (**4** - BF$_4$ - pyridine): 457.115, 459.117. Found: m/z = 457.351, 459.351. Crystal data [CCDC-961097]: C$_{20}$H$_{28}$BClF$_4$IrN$_3$ (**4**), M = 624.941, monoclinic, P2$_1$/c, a = 8.9512(10) Å, b = 24.437(3) Å, c = 10.4956(11) Å, β = 95.799(7)°, V = 2284.1(4) Å^3, Z = 4, d$_{calc}$ = 1.817 g/cm^3, T = 223 K, 21642 reflections collected, 5195 independent reflections (R_{int} = 0.0747), final R_1 = 0.0490, final wR_2 = 0.0567, GOF = 1.066.

[(η^5-pentamethylcyclopentadienyl)Ir^{III}bis-(κN-pyridine)Cl]BF$_4$ (5). [Cp*IrCl$_2$]$_2$ (80 mg, 0.1 mmol) was dissolved in CH$_2$Cl$_2$ (5 mL) and pyridine (32 mg, 0.4 mmol) added, causing an immediate color change from orange to yellow. Upon addition of AgBF$_4$ (39 mg, 0.2 mmol) in MeOH (1 mL) a colorless solid precipitated instantly. After stirring at room temperature for 15 minutes the solid was filtered off, discarded, and the clear solution dried *in vacuo* to leave a yellow solid. Recrystallization from CH$_2$Cl$_2$/Et$_2$O gave bright yellow microcrystals. Yield = 108 mg (89 %). ^{1}H-NMR (400 MHz, CD$_2$Cl$_2$): δ = 8.95 (d, J = 5.1 Hz, 4H, *o*-CH^{py}), 7.91 (t, J = 7.6 Hz, 2H, *p*-CH^{py}), 7.54 (t, J = 7.0 Hz, 4H, *m*-CH^{py}), 1.49 (s, 15H, C$_5$(CH_3)$_5$). ^{13}C{^{1}H}-NMR (100 MHz, CD$_2$Cl$_2$): δ = 153.3 (s, *o*-CH^{py}), 139.9 (s, *p*-CH^{py}), 127.5 (s, *m*-CH^{py}), 89.0 (s, *C$_5$*(CH$_3$)$_5$), 8.6 (s, C$_5$(*C*H$_3$)$_5$). ESI(+)MS calcd for C$_{15}$H$_{20}$ClIrN$^+$ (**5** - BF$_4$ - pyridine): 440.089, 442.091. Found: m/z = 440.081, 442.082. Crystal data [CCDC-961098]:

$C_{20}H_{25}BClF_4IrN_2$ (**5**), M = 607.910, monoclinic, P2$_1$/c, a = 9.2867(17) Å, b = 14.334(3) Å, c = 16.829(3) Å, β = 90.266(5)°, V = 2240.1(7) Å^3, Z = 4, d$_{calc}$ = 1.802 g/cm^3, T = 223 K, 14993 reflections collected, 4952 independent reflections (R_{int} = 0.0374), final R_1 = 0.0336, final wR_2 = 0.0661, GOF = 1.083.

[(η^5-pentamethylcyclopentadienyl)Ir^{III}bis-(κC-1,3-dimethylimidazol-2-ylidene)Cl]BF$_4$ (**6**).

[Ag(IMe)$_2$]BF$_4$ was prepared as a colorless crystalline solid from [1,3-dimethylimidazolium]BF$_4$, NaOH, and Ag$_2$O as described previously.[25] [Cp*IrCl$_2$]$_2$ (159 mg, 0.2 mmol) and [Ag(IMe)$_2$]BF$_4$ (155 mg, 0.4 mmol) were dissolved in dry CH$_2$Cl$_2$ (10 mL), and the resulting orange suspension stirred for one hour at room temperature. The colorless precipitate was filtered off, the solution concentrated to ~4 mL under reduced pressure, and filtered again through 0.2 μm pore size Teflon filter. Addition of Et$_2$O (15 mL) caused precipitation of a yellow-orange powder, which was collected and dried *in vacuo*. Yield = 234 mg (91 %). ^{1}H-NMR (400 MHz, CD$_2$Cl$_2$): δ = 7.08 (s, 4H, NC*H*C*H*N), 3.44 (s, 12H, NC*H$_3$*), 1.64 (s, 15H, C$_5$(C*H$_3$*)$_5$). ^{13}C{^{1}H}-NMR (100 MHz, CD$_2$Cl$_2$): δ = 147.5 (s, N*C*N), 124.4 (s, N*C*H*C*HN), 96.1 (s, *C$_5$*(CH$_3$)$_5$), 38.6 (s, N*C*H$_3$), 10.6 (s, C$_5$(*C*H$_3$)$_5$). ESI(+)MS calcd for $C_{20}H_{31}ClIrN_4^+$ (**6** - BF$_4$): 553.184, 555.186. Found: m/z = 553.117, 555.126. Crystal data [CCDC-961595]: $C_{20}H_{31}BClF_4IrN_4$ (**6**), M = 641.972, monoclinic, P2$_1$/n, a = 9.6053(10) Å, b = 17.4146(17) Å, c = 14.7645(15) Å, β = 102.613(3)°, V = 2410.1(4) Å^3, Z = 4, d$_{calc}$ = 1.769 g/cm^3, T = 223 K, 24506 reflections collected, 5484 independent reflections (R_{int} = 0.0397), final R_1 = 0.0405, final wR_2 = 0.0834, GOF = 1.075.

[(η^5-pentamethylcyclopentadienyl)Ir^{III}bis-(κC-1,4-dimethyl-1,2,4-triazol-5-ylidene)Cl]BF$_4$ (**7**).

[Ag(TMe)$_2$]BF$_4$ was prepared as a colorless crystalline solid from [1,4-dimethyl-1,2,4-triazolium]BF$_4$, NaOH, and Ag$_2$O as described previously for imidazole-2-ylidenes.[25] [Cp*IrCl$_2$]$_2$ (80 mg, 0.1 mmol) and [Ag(TMe)$_2$]BF$_4$ (78 mg, 0.2 mmol) were dissolved in dry CH$_2$Cl$_2$ (5 mL), and the resulting orange suspension stirred for six hours at room temperature. The colorless precipitate was filtered off, the solution concentrated to ~2 mL under reduced pressure, and filtered again through 0.2 μm pore size

Teflon filter. Addition of Et$_2$O (10 mL) caused precipitation of a yellow-orange powder, which was collected and dried *in vacuo*. Yield = 113 mg (88 %). ^{1}H-NMR (400 MHz, CD$_2$Cl$_2$): δ = 8.22 (s, 2H, NC*H*N), 3.85 (s, 6H, NC*H$_3$*), 3.40 (s, 6H, NC*H$_3$*), 1.70 (s, 15H, C$_5$(C*H$_3$*)$_5$). ^{13}C{^{1}H}-NMR (125 MHz, CD$_2$Cl$_2$): δ = 151.4 (s, N*C*N), 145.7 (s, N*C*HN), 96.5 (s, *C*$_5$(CH$_3$)$_5$), 40.3 (s, N*C*H$_3$), 35.5 (s, N*C*H$_3$), 10.1 (s, C$_5$(*C*H$_3$)$_5$). ESI(+)MS calcd for C$_{18}$H$_{29}$ClIrN$_6$$^+$ (**7** - BF$_4$): 555.174, 557.177. Found: m/z = 555.411, 557.399. Crystal data [CCDC-961099]: C$_{20}$H$_{20}$BClF$_4$IrN$_6$ (**7**), M = 658.898, triclinic, P-1, a = 9.5222(17) Å, b = 10.0943(18) Å, c = 12.105(2) Å, α = 88.626(5)°, β = 81.821(5)°, γ = 87.868(5)°, V = 1150.7(4) Å^3, Z = 2, d$_{calc}$ = 1.902 g/cm^3, T = 223 K, 11267 reflections collected, 4849 independent reflections (R_{int} = 0.0367), final R_1 = 0.0410, final wR_2 = 0.0710, GOF = 1.155.

[(η^5-pentamethylcyclopentadienyl)Ir^{III}bis-(κC-1,3-dimethylimidazol-2-ylidene)H]BF$_4$ (6-H). 6 (128 mg, 0.2 mmol) and NaBH$_4$ (76 mg, 2 mmol) were placed in a flame-dried Schlenk flask under N$_2$ and dry *iso*-propanol (10 mL) was added. The mixture was sonicated for five minutes and then stirred for another hour at room temperature. All volatiles were removed under reduced pressure to leave a beige solid, which was dried further *in vacuo*. The residue was extracted with CH$_2$Cl$_2$ (6 mL), the extract filtered through 0.2 μm pore size Teflon filter, and the pale yellow solution reduced to ~3 mL volume under reduced pressure. Addition of Et$_2$O (10 mL) caused precipitation of a very fine colorless solid, which was collected, washed with Et$_2$O (4 mL), and dried *in vacuo*. Yield = 110 mg (91 %). ^{1}H-NMR (500 MHz, CD$_2$Cl$_2$): δ = 7.02 (s, 4H, NC*H*C*H*N), 3.54 (s, 12 H, NC*H$_3$*), 1.93 (s, 15H, C$_5$(C*H$_3$*)$_5$), -16.24 (s, 1H, Ir*H*). ^{13}C{^{1}H}-NMR (125 MHz, CD$_2$Cl$_2$): δ = 149.9 (d, *J* = 5.2 Hz, N*C*N), 121.9 (s, N*C*HC*H*N), 92.8 (s, *C*$_5$(CH$_3$)$_5$), 39.1 (s, N*C*H$_3$), 10.5 (s, C$_5$(*C*H$_3$)$_5$). ESI(+)MS calcd for C$_{20}$H$_{32}$IrN$_4$$^+$ (**6-H** - BF$_4$): 519.223, 521.225. Found: m/z = 519.219, 521.223.

[(η^5-pentamethylcyclopentadienyl)Ir^{III}(κC,κC'-1,1'-methylene-bis(3-methylimidazolidin-2-ylidene))H]BF$_4$ (8-H). This compound has previously been obtained via a different synthetic route.[27] **8** (78 mg, 0.1 mmol) and AgPF$_6$ (26 mg, 0.11 mmol) placed in a flame-dried Schlenk flask under N$_2$ and

MeCN added (3 mL). NaBH$_4$ (38 mg, 1 mmol) and iso-propanol were then added, and the mixture stirred at 50 ˚C for two hours. After cooling to room temperature the mixture was filtered, and the pale yellow solution taken to dryness *in vacuo*. The solid residue was extracted with CH$_2$Cl$_2$ (4 mL) and filtered through 0.2 μm pore size Teflon filter. Addition of Et$_2$O (12 mL) caused precipitation of a pale yellow powder, which was collected, washed with Et$_2$O (3 mL), and dried *in vacuo*. Yield = 39 mg (60 %). ^{1}H-NMR (400 MHz, CD$_2$Cl$_2$): δ = 7.36 (d, J = 1.8 Hz, 2H, NC*H*CHN), 6.99 (d, J = 1.8 Hz, 2H, NCHC*H*N), 6.15 (d, J = 12.7 Hz, 1H, NC*H$_2$*N), 5.36 (d, J = 12.7 Hz, 1H, NC*H$_2$*N), 3.57 (s, 6H, NC*H$_3$*), 2.00 (s, 15H, C$_5$(C*H$_3$*)$_5$), -15.98 (s, 1H, Ir*H*).

Iridium(0) Nanoparticles. 2-3 nm Ir NPs were prepared using an adaption of a reported method.[48] [(coe)$_2$IrCl]$_2$ (9 mg, 0.01 mmol) in dry iso-propanol (3 mL) was stirred under an atmosphere of H$_2$ at 60 ºC until a greyish solution was obtained (15-30 minutes). At this point the atmosphere was exchanged to N$_2$, and the solution directly used for transfer-hydrogenation catalysis.

Catalysis. All complexes used in catalysis were freshly purified prior to use. Complexes **8**[27] and **9**[62] were purified by recrystallization from chloroform at -78 °C, and complex **14**[30] by column chromatography as described in the original publications. All others were purified by dissolution in a minimum amount of CH$_2$Cl$_2$, filtration through hydrophobic 0.2 μm Teflon filter, and recrystallization by addition of Et$_2$O as described in the synthesis part. Catalytic runs were performed by charging a flame-dried Schlenk flask with 20 μmol Ir-complex and 0.2 mmol 1,3,5-trimethoxybenzene (TMB) as internal standard under N$_2$ and adding 2 mL dry *iso*-propanol. After heating to the desired reaction temperature liquid substrate (2 mmol acetophenone) and base (0.2 mmol KOH, semiconductor grade) were added in 1 mL dry iso-propanol to start the reaction. Aliquots were withdrawn by syringe and quenched by mixing with CDCl$_3$ in air at room temperature. After filtration through celite the solution was analyzed for conversion by ^{1}H NMR. *In-situ* NMR reaction progress monitoring was performed in screw-capped 5 mm tubes, charged with solid iridium complex (0.007 mmol) and 1,3,5-

trimethoxybenzene (0.067 mmol) under N_2. A solution of KOH (0.067 mmol) in dry *iso*-propanol (1 mL) was added, followed by acetophenone (78 µL, 0.67 mmol). The NMR tube was sonicated for 30 seconds, placed in the NMR spectrometer with the probe preheated to 60 ºC, and ^{1}H NMR spectra acquired every 2 minutes.

SUPPORTING INFORMATION AVAILABLE

Details of crystallographic analyses, CIF files, original NMR spectra of all compounds tested in catalysis, and variable-temperature NMR data. This material is available free of charge via the Internet at http://pubs.acs.org.

REFERENCES

(1)   Klomp, D.; Hanefeld, U.; Peters, J. A. In *The Handbook of Homogeneous Hydrogenation*; Vries, J. G. d., Elsevier, C. J., Eds.; Wiley-VCH: Weinheim, **2007**; Vol. 3, p 585-630.

(2)   Bullock, R. M. *Chem. Eur. J.* **2004**, *10*, 2366-2374.

(3)   Guillena, G.; Ramón, D. J.; Yus, M. *Angew. Chem. Int. Ed.* **2007**, *46*, 2358-2364.

(4)   Nixon, T. D.; Whittlesey, M. K.; Williams, J. M. J. *Dalton Trans.* **2009**, 753-762.

(5)   Dobereiner, G. E.; Crabtree, R. H. *Chem. Rev.* **2009**, *110*, 681-703.

(6)   Watson, A. J. A.; Williams, J. M. J. *Science* **2010**, *329*, 635-636.

(7)   Haddad, Y. M. Y.; Henbest, H. B.; Husbands, J.; Mitchell, T. R. B. *Proc. Chem. Soc.* **1964**, 361.

(8)   Trocha-Grimshaw, J.; Henbest, H. B. *Chem. Commun.* **1967**, 544.

(9)   Henbest, H. B.; Mitchell, T. R. B. *J. Chem. Soc. C* **1970**, 785-791.

(10)   Camus, A.; Mestroni, G.; Zassinovich, G. *J. Mol. Catal.* **1979**, *6*, 231-233.

(11)   Suzuki, T. *Chem. Rev.* **2011**, *111*, 1825-1845.

(12)   Murata, K.; Ikariya, T.; Noyori, R. *J. Org. Chem.* **1999**, *64*, 2186-2187.

(13)   Fujita, K.-i.; Yamaguchi, R. *Synlett* **2005**, *4*, 560-571.

(14)   Zassinovich, G.; Mestroni, G.; Gladiali, S. *Chem. Rev.* **1992**, *92*, 1051-1069.

(15)   Palmer, M. J.; Wills, M. *Tetrahedron: Asymmetry* **1999**, *10*, 2045-2061.

(16)   Ikariya, T.; Blacker, A. J. *Acc. Chem. Res.* **2007**, *40*, 1300-1308.

(17)   Saidi, O.; Williams, J. M. J. *Top. Organomet. Chem.* **2011**, *34*, 77-106.

(18)   Hanasaka, F.; Fujita, K.-i.; Yamaguchi, R. *Organometallics* **2005**, *24*, 3422-3433.

(19)   Corberán, R.; Peris, E. *Organometallics* **2008**, *27*, 1954-1958.

(20)   Gnanamgari, D.; Sauer, E. L. O.; Schley, N. D.; Butler, C.; Incarvito, C. D.; Crabtree, R. H. *Organometallics* **2009**, *28*, 321-325.

(21)   Berliner, M. A.; Dubant, S. p. P. A.; Makowski, T.; Ng, K.; Sitter, B.; Wager, C.; Zhang, Y. *Org. Process Res. Dev.* **2011**, *15*, 1052-1062.

(22)   Pàmies, O.; Bäckvall, J.-E. *Chem. Eur. J.* **2001**, *7*, 5052-5058.

(23)   Samec, J. S. M.; Backvall, J.-E.; Andersson, P. G.; Brandt, P. *Chem. Soc. Rev.* **2006**, *35*, 237-248.

(24)   Cp*Ir complexes bearing functional Noyori-type ligands have been investigated more thoroughly (see for example: Arita S., Koike T., Kayaki Y., Ikariya T., *Organometallics* **2008**, *27*, 2795-2802; Pannetier N., Sortais J-B., Issenhut J-T., Barloy L., Sirlin C., Holuigue A., Lefort L., Panella L., de Vries J. G., Pfeffer M., *Adv. Synth. Catal.* **2011**, *353*, 2844-2852; Cross W. B., Daly C. G., Boutadla Y., Singh K., *Dalton Trans.* **2011**, *40*, 9722-9730; O W. W. N., Lough A. J., Morris R. H., *Organometallics* **2012**, *31*, 2152-2165).

(25)   Hintermair, U.; Englert, U.; Leitner, W. *Organometallics* **2011**, *30*, 3726-3731.

(26)   Xiao, X.-Q.; Jin, G.-X. *J. Organomet. Chem.* **2008**, *693*, 3363-3368.

(27)   Vogt, M.; Pons, V.; Heinekey, D. M. *Organometallics* **2005**, *24*, 1832-1836.

(28)   Ziessel, R. *J. Chem. Soc., Chem. Commun.* **1988**, 16-17.

(29)   Li, L.; Brennessel, W. W.; Jones, W. D. *J. Am. Chem. Soc.* **2008**, *130*, 12414-12419.

(30)   Brewster, T. P.; Blakemore, J. D.; Schley, N. D.; Incarvito, C. D.; Hazari, N.; Brudvig, G. W.; Crabtree, R. H. *Organometallics* **2011**, *30*, 965-973.

(31)   Ziessel, R.; Youinou, M.-T.; Balegroune, F.; Grandjean, D. *J. Organomet. Chem.* **1992**, *441*, 143-154.

(32)   Robertson, A.; Matsumoto, T.; Ogo, S. *Dalton Trans.* **2011**, *40*, 10304-10310.

(33)   Polshettiwar, V.; Varma, R. S. *Green Chem.* **2009**, *11*, 1313-1316.

(34)   Ouali, A.; Majoral, J.-P.; Caminade, A.-M.; Taillefer, M. *ChemCatChem* **2009**, *1*, 504-509.

(35)   Miecznikowski, J. R.; Crabtree, R. H. *Organometallics* **2004**, *23*, 629-631.

(36)   Allen, L. J.; Crabtree, R. H. *Green Chem.* **2010**, *12*, 1362-1364.

(37)   Johnstone, R. A. W.; Wilby, A. H.; Entwistle, I. D. *Chem. Rev.* **1985**, *85*, 129-170.

(38)   Hammond, C.; Schümperli, M. T.; Conrad, S.; Hermans, I. *ChemCatChem* **2013**, *5*, 2983–2990.

(39)   Kantam, M. L.; Reddy, R. S.; Pal, U.; Sreedhar, B.; Bhargava, S. *Adv. Synth. Catal.* **2008**, *350*, 2231-2235.

(40)   Alonso, F.; Riente, P.; Yus, M. *Tetrahedron Lett.* **2008**, *49*, 1939-1942.

(41)   Verho, O.; Nagendiran, A.; Johnston, E. V.; Tai, C.-w.; Bäckvall, J.-E. *ChemCatChem* **2013**, *5*, 612-618.

(42)   Alonso, F.; Riente, P.; Rodríguez-Reinoso, F.; Ruiz-Martínez, J.; Sepúlveda-Escribano, A.; Yus, M. *J. Catal.* **2008**, *260*, 113-118.

(43)   Subramanian, T.; Pitchumani, K. *Catal. Sci. Technol.* **2012**, *2*, 296-300.

(44)   Su, F.-Z.; He, L.; Ni, J.; Cao, Y.; He, H.-Y.; Fan, K.-N. *Chem. Commun.* **2008**, 3531-3533.

(45)   Sonnenberg, J. F.; Coombs, N.; Dube, P. A.; Morris, R. H. *J. Am. Chem. Soc.* **2012**, *134*, 5893-5899.

(46)   Toubiana, J.; Sasson, Y. *Catal. Sci. Technol.* **2012**, *2*, 1644-1653.

(47)   Crabtree, R. H. *Chem. Rev.* **2012**, *112*, 1536-1554.

(48)   Fonseca, G. S.; Scholten, J. D.; Dupont, J. *Synlett* **2004**, *2004*, 1525-1528.

(49)   Foley, P.; DiCosimo, R.; Whitesides, G. M. *J. Am. Chem. Soc.* **1980**, *102*, 6713-6725.

(50)   Widegren, J. A.; Finke, R. G. *J. Mol. Catal. A: Chem.* **2003**, *198*, 317-341.

(51)   Dröge, T.; Glorius, F. *Angew. Chem. Int. Ed.* **2010**, *49*, 6940-6952.

(52)   As we observed the formation of a colorless precipitate under reaction conditions we suspect a solubility limitation of the active species to cause the observed saturation. Unfortunately, these in-situ formed solids eluded characterization as they quickly changed color upon attempted isolation.

(53)   Gilbert, T. M.; Bergman, R. G. *J. Am. Chem. Soc.* **1985**, *107*, 3502-3507.

(54)   Glueck, D. S.; Winslow, L. J. N.; Bergman, R. G. *Organometallics* **1991**, *10*, 1462-1479.

(55)   Pons, V.; Heinekey, D. M. *J. Am. Chem. Soc.* **2003**, *125*, 8428-8429.

(56)   Campos, J.; López−Serrano, J.; Álvarez, E.; Carmona, E. *J. Am. Chem. Soc.* **2012**, *134*, 7165-7175.

(57)   Abura, T.; Ogo, S.; Watanabe, Y.; Fukuzumi, S. *J. Am. Chem. Soc.* **2003**, *125*, 4149-4154.

(58)   Hu, Y.; Li, L.; Shaw, A. P.; Norton, J. R.; Sattler, W.; Rong, Y. *Organometallics* **2012**, *31*, 5058-5064.

(59)   Furthermore, the test assumes that active monohydride intermediates do not engage in exchange mechanisms.

(60)   Wilkes, J. S.; Zaworotko, M. J. *J. Chem. Soc., Chem. Commun.* **1992**, 965-967.

(61)   Ball, R. G.; Graham, W. A. G.; Heinekey, D. M.; Hoyano, J. K.; McMaster, A. D.; Mattson, B. M.; Michel, S. T. *Inorg. Chem.* **1990**, *29*, 2023-2025.

(62)   Parent, A. R.; Brewster, T. P.; De Wolf, W.; Crabtree, R. H.; Brudvig, G. W. *Inorg. Chem.* **2012**, *51*, 6147-6152.